Coupling of organic and inorganic aerosol systems and the effect on gas–particle partitioning in the southeastern US

Havala O. T. Pye[1], **Andreas Zuend**[2], **Juliane L. Fry**[3], **Gabriel Isaacman-VanWertz**[4,5], **Shannon L. Capps**[6], **K. Wyat Appel**[1], **Hosein Foroutan**[1,7], **Lu Xu**[8], **Nga L. Ng**[9,10], and **Allen H. Goldstein**[5,11]

[1]National Exposure Research Laboratory, US Environmental Protection Agency, Research Triangle Park, North Carolina, USA

[2]Department of Atmospheric and Oceanic Sciences, McGill University, Montreal, Québec, Canada

[3]Department of Chemistry, Reed College, Portland, Oregon, USA

[4]Department of Civil and Environmental Engineering, Virginia Polytechnic Institute and State University, Blacksburg, Virginia, USA

[5]Department of Environmental Science, Policy, and Management, University of California, Berkeley, California, USA

[6]Civil, Architectural, and Environmental Engineering, Drexel University, Philadelphia, Pennsylvania, USA

[7]Department of Biomedical Engineering and Mechanics, Virginia Polytechnic Institute and State University, Blacksburg, Virginia, USA

[8]Department of Environmental Science and Engineering, California Institute of Technology, Pasadena, California, USA

[9]School of Chemical and Biomolecular Engineering, Georgia Institute of Technology, Atlanta, Georgia, USA

[10]School of Earth and Atmospheric Sciences, Georgia Institute of Technology, Atlanta, Georgia, USA

[11]Department of Civil and Environmental Engineering, University of California, Berkeley, California, USA

Abstract

Correspondence: Havala O. T. Pye (pye.havala@epa.gov).

Several models were used to describe the partitioning of ammonia, water, and organic compounds between the gas and particle phases for conditions in the southeastern US during summer 2013. Existing equilibrium models and frameworks were found to be sufficient, although additional improvements in terms of estimating pure-species vapor pressures are needed. Thermodynamic model predictions were consistent, to first order, with a molar ratio of ammonium to sulfate of approximately 1.6 to 1.8 (ratio of ammonium to 2× sulfate, $R_{N/2S} \approx 0.8$ to 0.9) with approximately 70% of total ammonia and ammonium (NH_x) in the particle. Southeastern Aerosol Research and Characterization Network (SEARCH) gas and aerosol and Southern Oxidant and Aerosol Study (SOAS) Monitor for AeRosols and Gases in Ambient air (MARGA) aerosol measurements were consistent with these conditions. CMAQv5.2 regional chemical transport model predictions did not reflect these conditions due to a factor of 3 overestimate of the nonvolatile cations. In addition, gas-phase ammonia was overestimated in the CMAQ model leading to an even lower fraction of total ammonia in the particle. Chemical Speciation Network (CSN) and aerosol mass spectrometer (AMS) measurements indicated less ammonium per sulfate than SEARCH and MARGA measurements and were inconsistent with thermodynamic model predictions. Organic compounds were predicted to be present to some extent in the same phase as inorganic constituents, modifying their activity and resulting in a decrease in $[H^+]_{air}$ (H^+ in $\mu g m^{-3}$ air), increase in ammonia partitioning to the gas phase, and increase in pH compared to complete organic vs. inorganic liquid–liquid phase separation. In addition, accounting for nonideal mixing modified the pH such that a fully interactive inorganic–organic system had a pH roughly 0.7 units higher than predicted using traditional methods (pH = 1.5 vs. 0.7). Particle-phase interactions of organic and inorganic compounds were found to increase partitioning towards the particle phase (vs. gas phase) for highly oxygenated (O : C 0.6) compounds including several isoprene-derived tracers as well as levoglu-cosan but decrease particle-phase partitioning for low O: C, monoterpene-derived species.

1 Introduction

Ambient particles consist of organic and inorganic compounds. The organic compounds present in the gas and particle phase are diverse and numerous (Goldstein and Galbally, 2007), ranging from relatively unoxidized, long-chain alkanes in fresh emissions to small, highly soluble compounds formed through multiple generations of atmospheric chemistry. Major inorganic constituents include water, sulfate, ammonium, and nitrate with additional contributions from species such as calcium, potassium, magnesium, sodium, and chloride (Reff et al., 2009). The extent to which organic and inorganic components of particulate matter interact within a particle depends on the mixing state (e.g., internal vs. external) of the aerosol population as well as the degree of phase separation (or number of phases) within the particle. Internally mixed populations, as typically assumed in chemical transport models such as the Community Multiscale Air Quality (CMAQ) model, may exhibit one fairly homogeneous liquid phase state or be heterogeneous in composition. Heterogeneous configurations occur as a result of phase separation and may include a liquid and solid phase or multiple liquid phases. A common heterogeneous configuration under conditions of liquid–liquid or solid–liquid phase separation is that of a core-shell morphology; alternatively, partially engulfed morphologies have been predicted by theory and observed in laboratory experiments (Kwamena et al., 2010; Song et al., 2013; Reid et al., 2011).

Currently, the CMAQ model, as well as other chemical transport models, considers accumulation-mode aerosol to form a heterogeneous internal mixture in which organic and inorganic constituents partition between the gas and aerosol phases independently of each other. Pye et al. (2017) examined how assumptions about phase separation of internally mixed particles affect organic aerosol concentrations in the southeastern US as predicted by the CMAQ model. When organic compounds were allowed to mix with the aqueous inorganic phase under conditions of high relative humidity and a high degree of oxygenation (You et al., 2013; Bertram et al., 2011; Song et al., 2012), the concentration of organic aerosol was predicted to increase significantly (Pye et al., 2017). While the effects of phase separation on organic compounds are potentially large, they are highly dependent on an accurate parameterization of activity coefficients and a reliable prediction of the composition of individual particle phases (Zuend and Seinfeld, 2012).

Recent work highlights potential discrepancies between current gas–particle partitioning models, which assume equilibrium is attained on short timescales, and observations for both inorganic and organic compounds. Silvern et al. (2017) found that models predict higher ratios of particulate ammonium to sulfate than observed in the eastern US and proposed that organic compounds in an organic-rich phase at the particle surface may reduce ammonia partitioning to the particle via a kinetic inhibition. In addition, organic compound vapor pressure estimation method predictions can vary by orders of magnitude (Topping et al., 2016; O'Meara et al., 2014; Pankow and Asher, 2008) and have often been adjusted downward to improve model predictions (Chan et al., 2009; Johnson et al., 2006). Furthermore, isoprene-epoxydiol-derived organic aerosol partitions to the particle phase to a greater degree than structure-based vapor pressures would suggest (Isaacman-VanWertz et al., 2016; Lopez-Hilfiker et al., 2016; Hu et al., 2016). Since $PM_{2.5}$ (particulate matter concentration from particles of diameters less than 2.5 μm) is regulated via the National Ambient Air Quality Standards (NAAQS) in the US, while similar ambient standards are not set for the gas-phase counterparts (NH_3 and organic compound vapors), errors in partitioning will affect model performance with implications for metrics used in regulatory applications. The model sensitivity of $PM_{2.5}$ to emission changes can also be too high or too low if compounds are erroneously partitioned.

In this work, gas–particle partitioning of ammonia and several isoprene-, monoterpene-, and biomass burningderived organic compounds was examined using common air quality modeling treatments and advanced approaches. Results address the degree to which techniques accounting for organic–inorganic interactions, deviations in ideality, and phase separation reproduce observations. Models were evaluated for their ability to predict ammonia vs. ammonium as well as gas–particle partitioning of organic compounds. In addition, the effects of organic compounds on aerosol pH were examined.

2 Methods

2.1 Model approaches

Several box model approaches as well as CMAQ regional chemical transport model calculations were used to represent the partitioning of compounds between the gas and particle phases. CMAQ version 5.2-gamma was run over the continental US at 12 km by 12

km horizontal resolution for 1 June–15 July 2013, coinciding with the Southern Oxidant and Aerosol Study (SOAS) field campaign and the Centreville, Alabama, US, field site. WRF v3.8 meteorology with lightning assimilated into the convection scheme (Heath et al., 2016) was processed for use with the CMAQ model (Otte and Pleim, 2010). Emissions were based on the 2011 National Emissions Inventory version 2 (ek). Emissions influenced by model meteorology (biogenic compounds, mobile sector) or monitored at the source (electrical generation units) were 2013 specific. Windblown dust emissions followed the scheme of Foroutan et al. (2017). Ammonia emissions and deposition from croplands were parameterized as a bidirectional exchange (Pleim et al., 2013). CMAQ used ISORROPIA v2.1 (Fountoukis and Nenes, 2007; Nenes et al., 1998) with gas and aerosol composition and environmental conditions (temperature, relative humidity) as input to predict the Aitken- and accumulation-mode ammonium, nitrate, and chloride mass concentrations. CMAQ-predicted PM_1 and $PM_{2.5}$ were computed based on the fraction of the Aitken and accumulation modes less than 1 or 2.5 μm in diameter as appropriate (Nolte et al., 2015).

Consistent with the CMAQ regional model, partitioning of ammonia between the gas and particle phases was also predicted using ISORROPIA as a box model driven with observed aerosol (reverse mode) or gas and aerosol (forward mode) concentrations of ammonia, ammonium, nitrate, nitric acid, calcium, potassium, magnesium, sodium, and chloride. Output from the ISORROPIA box model was either gasphase ammonia in equilibrium with the observed aerosol ammonium (reverse mode) or ammonia vs. ammonium based on total gas and aerosol conditions (forward mode). ISORROPIA does not consider the effects of organic compounds on aerosol pH or explicitly treat liquid–liquid phase separation.

Algorithms that allowed for inorganic–organic interactions were applied using a thermodynamic equilibrium gas–particle partitioning model (Zuend et al., 2010; Zuend and Seinfeld, 2012) based on the Aerosol Inorganic–Organic Mixtures Functional groups Activity Coefficients (AIOMFAC) model (Zuend et al., 2008, 2011). AIOMFAC provided an estimate of activity coefficients for aerosol systems of specified functional group composition, which was used in two modes: (i) predefined complete liquid–liquid phase separation (CLLPS) in which the organic compounds did not mix with the inorganic salts and (ii) equilibrium (EQLB) in which the Gibbs energy of the system was minimized and up to two liquid phases of any composition were allowed to form in the particle as predicted by a modified liquid–liquid phase separation algorithm based on the method by Zuend and Seinfeld (2013). For purposes of AIOMFAC calculations, observed calcium, potassium, and magnesium concentrations were converted to charge-equivalent sodium amounts since the former's interactions with the bisulfate ion in solution are not treated by the model.

Several quantities, including pH and molar ratios, were calculated to evaluate the inorganic aerosol system. Solution acidity can be expressed in different ways, the most common one being the pH value. However, many definitions of pH exist, with several definitions only applicable to highly dilute aqueous solutions. Thermodynamics-based pH definitions vary with the choice of composition scale (molality, molarity, or mole fraction basis) and the solvent into which H^+ is assumed to dissolve, which may be strictly water associated with inorganic constituents as in ISORROPIA II, or include the diluting effect of water associated with organic compounds (Guo et al., 2015), organic compounds themselves (Zuend et al.,

2008), or other aerosol constituents (Budisulistiorini et al., 2017). Furthermore, activity coefficients of H^+ may not be unity as is frequently assumed. In this work, pH was defined following the thermodynamic definition on a molality basis, as recommended by IUPAC (http://goldbook.iupac.org/html/P/P04524.html) and computed by the AIOMFAC model. By expressing the molality of H^+ in terms of concentration per volume of air, the following results:

$$\text{pH} = -\log_{10}(\gamma_{H+}[H^+]_{\text{air}}/[S]), \quad (1)$$

where γ_{H^+} is the molality-based activity coefficient for H^+ in the liquid phase, $[H^+]_{\text{air}}$ is the concentration of the hydronium ion in the liquid phase in moles per volume of air, and $[S]$ is the solvent mass in that liquid phase (kilogram per volume of air), i.e., $[H^+]_{\text{air}}=[S]$ is the molality of H^+ The solvent included water associated with inorganic compounds (W_i), water associated with organic compounds (W_o), and organic compounds (C_{org}) as appropriate based on the predicted phase composition. ISORROPIA pH calculations assumed $[S] = [W_i]$ and an activity coefficient of unity thus following previous methods (Guo et al., 2017a). The molar ratio of ammonium to $2 \times$ sulfate was defined as

$$R_{\text{N/2S}} = \frac{n_{NH_4^+}}{2 \times n_{SO_4^{2-}}}, \quad (2)$$

and the electric-charge-normalized molar ratio of cations to anions that participate in ISORROPIA was

$$R_{+/-} = \frac{n_{NH_4^+} + n_{Na^+} + 2 \times n_{Ca^{2+}} + n_{K^+} + 2 \times n_{Mg^{2+}}}{2 \times n_{SO_4^{2-}} + n_{NO_3^-} + n_{Cl^-}}. \quad (3)$$

Since ambient measurements and CMAQ model output do not distinguish bisulfate from sulfate, the sulfate in these ratios represented total sulfate $\left(SO_4^{2-} + HSO_4^-\right)$.

To employ the AIOMFAC-based equilibrium models, organic aerosol positive matrix factorization (PMF) analysis results of ambient data (next section) were converted to molecular structures of known functional group composition as surrogates for a range of organic compound classes in ambient particles as described in Tables S1–S3 in the Supplement thus providing a complete characterization of the organic aerosol partitioning medium. Several isoprene-derived (2-methyltetrols, C_5-alkene triols, 2-methylglyceric acid) and monoterpene-derived (pinic acid, pinonic acid, hydroxyglutaric acid) compounds as well as levoglucosan, a semivolatile indicator of biomass burning, were explicitly represented in box model calculations. Pure species' vapor pressures (sub-cooled liquid) were obtained via the EVAPORATION model (Compernolle et al., 2011). The temperature dependence was

parameterized by using the same Antoinelike function that is also employed by the EVAPORATION model. A sensitivity calculation (referred to as Adj Psat) reduced EVAPORATION-based vapor pressures by a factor of 4.2, thus maintaining the compound-to-compound variability predicted by EVAPORATION but correcting for potential overestimates in pure compound vapor pressures. The magnitude of the adjustment was based on the effective saturation concentration obtained via regression needed to reproduce observations in a traditional absorptive partitioning framework (Eq. S1). This adjustment factor is similar in magnitude to the difference between SIMPOL (Pankow and Asher, 2008) and EVAPORATION (Compernolle et al., 2011) predicted vapor pressures for several species, but not all (see Table S4). The effective saturation concentration, C^*, of a species, i, was defined as (Zuend and Seinfeld, 2012)

$$C_i^* = \frac{C_i^{\mathrm{g}} \sum C_k^{\mathrm{PM}}}{C_i^{\mathrm{PM}}}, \quad (4)$$

where C_i^{g} is the mass-based gas-phase concentration of species i, C_i^{PM} is the mass-based liquid-phase concentration of species i, and C_k^{PM} is the total mass-based concentration of the liquid phase where the summation index k includes organic species, inorganic species, and water. See Eq. (S2) for C_i^* in terms of the mole-fraction-based activity coefficient.

2.2 Ambient data

Regional model predictions of inorganic aerosol were evaluated against the Chemical Speciation Network (CSN) and Southeastern Aerosol Research and Characterization (SEARCH) network observations (at different ground sites). The Interagency Monitoring of Protected Visual Environments (IMPROVE) network (Solomon et al., 2014) also measures some chemical speciation of $PM_{2.5}$ throughout the US, but does not include ammonium. CSN determines anions and cations via ion chromatography of extracts from nylon filters (Solomon et al., 2014). Solomon et al. (2014) estimate the precision of CSN measured ammonium is 11% and sulfate is 7% (for co-located samples during 2012) but the actual measurement uncertainty is likely higher (and not quantified). The SEARCH network operates at fewer sites and exclusively in the southeastern US. It uses a multichannel approach employing nylon, teflon, and citric-acid-coated cellulose filters to measure speciated 24 h average $PM_{2.5}$ (Edgerton et al., 2005). SEARCH reports that the precision of measured sulfate and ammonium in $PM_{2.5}$ is 2–3% (Egerton et al., 2005). The SEARCH 24 h filter measurements are also used to adjust the co-located continuous measurements (Edgerton et al., 2006).

In addition to the network data, ambient data from SOAS at the Centreville, AL (CTR; 87.25° W, 32.90° N), site from June and July 2013 were used as input to the box models and for model evaluation. The high-resolution time-of-flight aerosol mass spectrometer (HR-ToF-AMS, hereafter AMS) operated by the Georgia Institute of Technology was the primary source of SOAS PM_1 organic mass, ammonium, and sulfate (Xu et al., 2015a). This AMS data set was consistent with the other AMS instrument operating at CTR as well as AMS

measurements aboard an aircraft over the southeastern US (Tables S5–S6). When AMS data were used as input in PM_1 box modeling, inorganic nitrate was set to zero as nitrate measured by the AMS contained significant contributions from compounds that contain organic nitrogen (Xu et al., 2015b). Thus, AMS calculations assumed the inorganic aerosol was composed only of ammonium, sulfate, bisulfate, and the hydronium ion (referred to in subsequent sections as the A' system). The assignment of measured ammonium and sulfate to specific salts (ammonium sulfate vs. ammonium bisulfate) for use as input electrolyte components to AIOMFAC was determined using mass balance. Inorganic $PM_{2.5}$, including ammonium, sulfate, nitrate, calcium, potassium, magnesium, sodium, and chloride, was measured at CTR with a Monitor for AeRosols and Gases in Ambient air (MARGA) (Allen et al., 2015). Less than 5% of the $PM_{2.5}$ MARGA data used in this work had elevated nitrate (> 0.8 μgm^{-3}) due to supermicron crustal material and sea salt episodes (Allen et al., 2015). The data from MARGA were used in two ways for model calculations with AIOMFAC. (1) All the measured ion concentrations were considered, but the molar amounts of the cations Ca^{2+}, K^+, Mg^{2+}, and Na^+ were mapped to a charge-equivalent amount of Na^+ (see Sect. 2.1). (2) Only the measured concentrations of ammonium and sulfate ions were considered and mapped to the electrolyte components ammonium sulfate, ammonium bisulfate, and sulfuric acid for AIOMFAC model input purposes. For ammonium-sulfate-only conditions (option 2) in which the moles $NH_4^+ \geq 2 \times SO_4^{2-}$, a small amount ($1 \times 10^{-4}$ μgm^{-3}) of ammonium bisulfate was added to the AIOMFAC input for MARGA calculations in order to trigger a potential partial association of sulfate and H^+ ions to bisulfate following the equilibrium constant of that reaction. Such conditions did not occur with AMS data. Hourly gas-phase ammonia was obtained from the CTR SEARCH network site via a corrected Thermo Scientific citric-acidimpregnated denuder. Relative humidity (RH) and temperature were obtained from the routine SEARCH network measurements at the SOAS site.

The entire organic aerosol composition was characterized in terms of functional groups for use with AIOMFAC. The semi-volatile thermal desorption aerosol gas chromatograph (SV-TAG) with in situ derivatization (Isaacman-VanWertz et al., 2016; Isaacman et al., 2014) provided measured gas- and aerosol-phase concentrations of 2-methyltetrols, C_5-alkene triols, 2-methylglyceric acid, pinic acid, pinonic acid, hydroxyglutaric acid, and levoglucosan. More-oxidized oxygenated organic aerosol (MO-OOA), biomass burning organic aerosol (BBOA), isoprene OA, and less-oxidized oxygenated organic aerosol (LO-OOA) PMF factors from the AMS were represented with specific functional groups and associated surrogate chemical structures (Table S1). As previous work indicates that a fraction of measured 2-methyltetrols may be decomposition products of lowvolatility accretion products (Isaacman-VanWertz et al., 2016; Lopez-Hilfiker et al., 2016), 50% (as a rough estimate) of measured 2-methyltetrols (in the particle phases) were assumed to be dimer decomposition products when EVAPORATION-based vapor pressures were used (see Table S4). In the sensitivity calculation (Adj Psat), 2-methyltetrols were assumed to be present only in the monomer form as including dimers increased the model bias.

The overlap in the input data sets resulted in 180 h of measurement coverage. Additional measurements of ammonium, sulfate, and ammonia (not used in this work) are summarized in Tables S5–S7 for reference.

3 Results and discussion

3.1 Regional ammonium sulfate conditions

Figure 1 shows the molar ratios of ammonium to $2 \times$ total sulfate and cations to anions over the eastern US for 1 June–15 July 2013 based on observations from the CSN network and predicted by CMAQv5.2. CMAQ predicted a mean $R_{N/2S}$ of 0.73 over the US compared to the observed mean of 0.67. The model showed higher values (near 1) over the central US and lower values over the southeastern US. The magnitude of the CMAQ-predicted $R_{N/2S}$ over the southeastern US (mean of 0.6) was only slightly higher than that from the CSN network (mean of 0.4). CMAQ-predicted sulfate was relatively unbiased in the southeastern US (normalized mean bias of 5% compared to CSN), but ammonium was high by a factor of 1.5 (Table S10). Despite only a moderate bias in $R_{N/2S}$, significant discrepancies existed between the model and observations for the ratio of cations to anions. In CMAQ, the ratio of cations to anions was approximately 1, indicating that ammonia tended to be pulled into the particle in an amount necessary to neutralize sulfate not already associated with nonvolatile cations. Molar ratios are not robust indicators of aerosol pH (Hennigan et al., 2015) as a result of the role of RH and associated liquid water content as well as buffering by bisulfate (Guo et al., 2015). However, chemical transport model biases in ion ratios should result in biases in acidity and gas–particle partitioning of volatile acids and bases (e.g., NH_3) considering other factors (such as RH) held constant.

Also included in Fig. 1a are observations of $R_{N/2S}$ based on the SEARCH network (triangles) that are much higher (> 0.8) than the CSN values (< 0.6) in the southeastern US. While there could be spatial heterogeneity in the southeastern US, differences so large are unlikely and not present in CMAQ, thus indicating potential problems in one set of measurements. Nylon filters (used by CSN for inorganic ions) can collect 4–5% of gas-phase sulfur dioxide (Benner et al., 1991; Hansen et al., 1986), leading to a small but positive sulfate mass concentration artifact. In addition, nylon filters tend to measure lower ammonium concentrations than other filter types (Solomon et al., 2000; Yu et al., 2006). These ammonium artifacts are not restricted to ammonium nitrate since more than twice as much NH_4^+ was lost compared to nitrate on nylon filters from Great Smoky Mountains National Park, TN, US (Yu et al., 2006). Of total NH_4^+, 6–14% can volatilize in federal reference method (FRM) collection, and the SEARCH network best estimates of $PM_{2.5}$ result in higher ammonium on an absolute basis and as a fractional contribution to $PM_{2.5}$ compared to the FRM equivalent mass (Edgerton et al., 2005). Consider that a 10% underestimate in ammonium PM and a 10% overestimate in sulfate, for example, will lead to almost a 20% underestimate in $R_{N/2S}$.

An overabundance of cations in the CMAQ model (Fig. S1, Table S10 in the Supplement) means that ammonium was displaced from the particle and $R_{N/2S}$ was biased low for the southeastern US. An evaluation of the individual cations and anions (Fig. S1, Table S10) indicated CMAQ overpredicted the nonvolatile ISORROPIA cations (Na^+, Ca^{2+}, K^+, Mg^{2+}) by factors of 2 to 6 individually and by a charge equivalent factor of 3 overall in the southeast. A factor of 3 overestimate in nonvolatile cations indicates ammonium predicted by CMAQ was low by about 26 %. Appel et al. (2013) have previously shown that even

when anthropogenic fugitive dust and windblown dust emissions are removed from the CMAQ model, crustal elements are still typically overestimated compared to observations. Coal combustion, for example, is a major source of trace metals in the US (Reff et al., 2009). Trace metal emissions were overestimated (and/or physical mixing was underestimated) since CMAQ overestimated their measured concentration, which included soluble and insoluble contributions (Solomon et al., 2014). A sensitivity simulation in which all Aitken- and accumulation-mode Na^+, Ca^{2+}, K^+, and Mg^{2+} were removed from the partitioning thermodynamics resulted in a mean predicted $R_{N/2S}$ of 0.96 for the southeastern US. Since ISORROPIA should only consider the cations associated with sulfate, nitrate, and chloride but CMAQ includes cations that are part of insoluble metal oxides (Reff et al., 2009), additional error was incurred in CMAQ by allowing all of the calcium, potassium, magnesium, and sodium present in aerosol to participate in ISORROPIA calculations. Thus, the apparent consistency in ammonium-tosulfate ratios between CSN and CMAQ should not be used to confirm the reasonableness of either. The ratio of cations to anions indicates discrepancies between CSN and CMAQ, specifically, that the CMAQ model tends to achieve charge balance as defined by $R_{+/-} = 1$ while observations indicate otherwise.

3.2 Ammonia gas–particle partitioning during SOAS

Consistent with CMAQ predictions over the greater southeastern US region, CMAQ predicted an average ratio of ammonium to $2 \times$ sulfate ($R_{N/2S}$) of 0.64–0.61 (for PM_1 and $PM_{2.5}$, respectively) and 24–28% of total ammonia in the particle as ammonium (Fig. 2b and g) at CTR. CMAQ also predicted that the cation-to-anion charge ratio, $R_{+/-}$, was near 1 during SOAS. Thus, CMAQ predictions for the SOAS CTR site were representative of the southeastern US for further investigating CMAQ model issues related to inorganic molar ratios and ammonia partitioning.

As shown in Fig. 2, the CMAQ-predicted $R_{N/2S}$ (b) was similar to the value derived with the Georgia Tech AMS (a). It was also similar to the regional SEAC4RS (Studies of Emissions, Atmospheric Composition, Clouds, and Climate Coupling by Regional Surveys) AMS- derived values (Silvern et al., 2017) (Table S6), which averaged near 0.6. ISORROPIA predictions using AMS-measured ammonium and sulfate as input (c), thus exactly reproducing observed $R_{N/2S}$, showed much higher partitioning of ammonia to the particle phase (mean $NH_x F_p$ of 0.8) than indicated by AMS aerosol data combined with SEARCH ammonia. Using total ammonia and ammonium as model input resulted in a similar fraction of NH_x in the particle as using only aerosol composition as input, but the $R_{N/2S}$ value significantly increased to around 0.8 (d). The AIOMFAC-based equilibrium model run with aerosol-only inputs (e) was qualitatively consistent with ISORROPIA (c) in terms of the fraction of NH_x in the particle. Since no box model simulation of AMS data in this work was able to reproduce both the $NH_x F_p$ and $R_{N/2S}$, these tests indicated that AMS measurements at SOAS CTR were inconsistent with ISORROPIA and AIOMFAC thermodynamic calculations, as found in previous model evaluation (Silvern et al., 2017).

The $R_{N/2S}$ determined from the MARGA instrument for $PM_{2.5}$ (f) was significantly higher than that derived from the AMS measurements and closer to the values based on SEARCH measurements (Table S5, Fig. 1). The AMS tended to measure much less ammonium than

the MARGA, and as a result, the fraction of ammonia partitioned to the particle using SEARCH NH_3 and MARGA aerosol measurements was higher than would be estimated using AMS data. The CMAQ model calculations showed a small but similar trend to observations for PM_1 to $PM_{2.5}$ in terms of ammonia gas–particle partitioning (since $PM_{2.5}$ PM_1 and $F_p = PM/(PM+gas)$) but did not show significantly increased $R_{N/2S}$ with increased particle size. Note that in full CMAQ model calculations, the predicted nonvolatile cation concentrations were so high that they erroneously affected the partitioning of ammonium (Table S10, Fig. S1). Removing nonvolatile cations from CMAQ (h) allowed more ammonium into the particle and led to increased $R_{N/2S}$, but $NH_x F_p$ was still low, indicating that overestimates in gas-phase ammonia in the CMAQ model are not primarily due to the displacement of ammonium by nonvolatile cations.

ISORROPIA $PM_{2.5}$ calculations using both gas and aerosol inputs were run with (j in Fig. 2) and without (k) aerosol calcium, potassium, magnesium, sodium, nitrate, and chloride and the results were qualitatively the same in terms of mean fraction of ammonia partitioned to the particle and ratio of NH_4^+ to sulfate in the particle. Thus, the difference between AMS and MARGA observations was primarily driven by the difference in ammonium and sulfate measured by the AMS vs. MARGA instrument, not the availability of nonvolatile cations. Comparing the change in mean $NH_x F_p$ with (m) and without (l) organic compound interactions indicates that organic compounds have a larger effect on ammonia gas–particle partitioning than the inclusion (j) or lack (k) of calcium, potassium, magnesium, sodium, nitrate, and chloride. Overall, ISORROPIA and AIOMFAC were qualitatively consistent with MARGA measurements of $R_{N/2S}$, but not with AMS measurements.

The inconsistency in AMS data and box models indicated in Fig. 2, but ability of models to simulate MARGA data, indicates the AMS data alone may not be suitable for equilibrium thermodynamic modeling. Contributing factors could include missing ammonium residing in particles larger than PM_1 but smaller than $PM_{2.5}$, potential missing nonvolatile cations, uncertainty in AMS-measured concentrations of sulfate and ammonium, organosulfate contributions to sulfate, or other issues. Guo (2017) indicates differences in ammonium-to-sulfate ratios for PM_1 measured during the first half of SOAS vs. $PM_{2.5}$ measured during the second half of SOAS using the same instrument (the Particle into Liquid Sampler, PILS; Guo et al., 2017b), suggesting a role of particle size in ammonium-to-sulfate ratios. Furthermore, thermodynamic predictions of ammonia were degraded in the work of Guo et al. (2015) when the PILS inlet switched from $PM_{2.5}$ to PM_1. Size alone does not explain the difference in AMS (PM_1) vs. $PM_{2.5}$ data as AMS sulfate can be similar to (MARGA) or exceed by 20% (PILS, Guo et al., 2015) collocated $PM_{2.5}$ sulfate. Future work that characterizes ammonium and sulfate in $PM_{2.5} - PM_1$ would be helpful for understanding differences in AMS vs. other data sets as well as to facilitate connections between AMS data and regulatory metrics including the US NAAQS for $PM_{2.5}$. Guo et al. (2017b) suggest when AMS (or PILS) data are used together with nonvolatile cations, thermodynamic models can predict ammonia partitioning accurately. However, MARGA simulations in this work (Fig. 2j and k) indicated little sensitivity of $R_{N/2S}$ or $NH_x F_p$ to inclusion of measured calcium, potassium, magnesium, sodium, nitrate, and chloride.

The differences in the AMS and MARGA data sets in terms of $R_{N/2S}$ are larger than can be explained by known measurement precision. However, uncertainty for AMSmeasured ammonium (34 %) and sulfate (36 %) is large (Bahreini et al., 2009). A contributor to this uncertainty is the AMS collection efficiency (CE), and AMS instruments are known to have a higher CE for acidic (H_2SO_4 enriched) vs. $(NH_4)_2SO_4$-enriched aerosol (Middlebrook et al., 2012). Furthermore, organosulfates (Budisulistiorini et al., 2015; Hettiyadura et al., 2017) can be measured in the AMS as sulfate. However, organosulfates have been estimated to account for only 5% of AMS-measured sulfate during SOAS (Hu et al., 2017).

3.3 Phase composition

Figure 3 shows the average concentration of aerosol components predicted in the electrolyte-rich (α) and organicrich (β) aerosol phases as well as under conditions in which only one liquid phase was predicted (single phase) based on AIOMFAC equilibrium calculations (EQLB) of the aqueous ammonium–sodium–sulfate–nitrate–chloride (A) and organic surrogates system. In all cases, water was predicted to be a major contributor to the phase, accounting for 60, 35, and 90% of the mass in the average α, β, and single phases, respectively. In addition, inorganic ions were present in all phases including the organic-rich phase. This means that the effects of inorganic species on organic compounds were not limited to times when one single liquid phase was predicted. Higher concentrations of organic species were generally associated with an increase in the predicted frequency of phase separation. However, LO-OOA, the least oxygenated (Table S2) and least water-soluble secondary organic aerosol PMF factor (Xu et al., 2017), was not more or less abundant when phase-separated vs. single-phase conditions were predicted.

The mean $R_{N/2S}$ varied slightly by phase, with the α phase having a value of 0.8 and the phases with a greater proportion of organic compounds (β and single) having a value of 0.9. The β phase, with its higher concentration of organic species, showed a lower average [H$^+$]$_{air}$ (0.1 nmolm^{-3}) compared to the α phase (1.5 nmolm^{-3}), while the activity-based pH values were predicted to be similar in both phases, typically within 0.2 pH units (as expected from equilibrium thermodynamics). The ammonium-sulfate-only (in terms of inorganic ion representation) system was predicted to have the same frequency of phase separation and trend in [H$^+$]$_{air}$, but less difference in the $R_{N/2S}$ between the phases.

Phase separation into electrolyte-rich and organic-rich phases was predicted to occur 70% of the time. The frequency of phase separation predicted for SOAS conditions was higher than the frequency predicted in previous CMAQ work (Pye et al., 2017) that calculated separation RHs based on average O : C ratios using the empirical parameterization of You et al. (2013) for a particular inorganic salt type. Both the previous CMAQ calculations (Pye et al., 2017) and this work predicted the same diurnal variation with a greater frequency of phase separation during the day driven by a lower RH (Fig. S7).

3.4 Effects of organic compounds on acidity

Acidity (pH) is an important aerosol property as it promotes dissolution of metals (Fang et al., 2017), increases nutrient availability (Stockdale et al., 2016), and catalyzes particle-phase reactions (Eddingsaas et al., 2010). Current recommended methods for estimating

aerosol pH include thermodynamic models and ammonia–ammonium partitioning (Hennigan et al., 2015) as direct measurements are difficult to make (Rindelaub et al., 2016). AIOMFAC predicted a median molal pH of 1.4 (ammonium–sulfate system) to 1.5 (ammonium–sodium–sulfate–nitrate–chloride system) for SOAS conditions (Table 1). AIOMFAC occasionally showed a high pH (pH D 7, Fig. 4), which occurred when an excess of cations compared to anions was observed, leading to the absence of H^+ and bisulfate in the input compositions used with the model. Similar behavior has occurred with ISORROPIA and the AIM thermodynamic models using aerosol-only inputs (Hennigan et al., 2015) and likely resulted from measurement uncertainty and a resulting highbias in the measured numbers of cations compared to chargeequivalent anions. The ISORROPIA-predicted pH for the subset of conditions used here (pH = 0.7 to 1.1) was similar to those previously reported for SOAS (pH = 0.9) and Southeast Nexus (SENEX) aircraft campaign (pH = 1.1) using other data sets as summarized by Guo et al. (2017a).

Regardless of whether only ammonium–sulfate or ammonium–sodium–sulfate–nitrate–chloride systems were treated, AIOMFAC predicted an increase in the concentration of gas-phase ammonia (decrease in NH_x F_p; Fig. 2m compared to l or o compared to n) along with a decrease in acidity when organic compounds were considered in the calculation of partitioning (EQLB vs. CLLPS; Table 1, Fig. 4). The presence of organic compounds in the same phase as H^+ and other ions (EQLB case) shifted free H_+ towards increased association with sulfate to form bisulfate as AIOMFAC predicts bisulfate to be more miscible with organic compounds than H^+ and other small cations. Interactions with organic compounds resulted in a 34–36% decrease in median $[H^+]_{air}$ and a 0.1 unit increase (11–12% increase) in median pH.

If the pH for forced complete phase separation conditions was recalculated using $[H^+]_{air}$ predicted with AIOMFAC CLLPS and assuming an activity coefficient of 1 (traditional method), the resulting pH has a median of 0.7 (Fig. 4b), the same value obtained by ISORROPIA using only aerosol inputs and an activity coefficient of unity. Thus, traditional methods resulted in an artificially low pH. Taking into account activity coefficients other than unity, phase separation, and the diluting effect of organic compounds and their associated water (EQLB) resulted in a pH 0.7 pH units higher than traditional methods. This increase is substantial given that the pH scale is logarithmic; a value 0.7 pH unit higher is equivalent to a molal H^+ activity in solution that is 5 times lower. The activity coefficient value was a major driver of this difference with a secondary role for solvent abundance and change in $[H^+]_{air}$.

3.5 Partitioning of organic compounds under ambient conditions

For organic compounds with O : C   0.6 (C_5-alkene triols, levoglucosan, 2-methyltetrols, hydroxyglutaric acid, 2- methylglyceric acid), the particle-phase fraction, F_p, was predicted to increase when the electrolyte-rich and organicrich phases were allowed to equilibrate (EQLB compared to CLLPS, Figs. 5 and 6) as a result of an increase in the abundance of the partitioning medium. For compounds with lower O : C (specifically pinic and pinonic acid) F_p decreased as a result of unfavorable liquid-phase interactions. The increase in F_p for most species generally resulted in a decrease in the mean bias and mean error of F_p compared to

observations (Fig. 5b). With the pure-species-adjusted vapor pressure (Adj Psat sensitivity), the mean bias in F_p for all organic species was less than 0.2 and emphasized that information about the pure-species vapor pressure is important for accurate gas–particle partitioning calculations. The influence of inorganic constituents on organic compound partitioning was not limited to the times when one single phase was present. In the case of hydroxyglutaric acid (Fig. 6g), predictions of F_p were found to be most sensitive to assumptions regarding condensed phase mixing during the day when phase separation was most common (coinciding with a lower average RH during midday and afternoon hours, as expected). This occurred because the organic-rich phase still contained a significant number of inorganic ions (Fig. 3), which modified the partitioning medium and impacted the predicted activity of the organic species.

The change in F_p between CLLPS and EQLB calculations was consistent with the change in effective saturation concentrations (Fig. 5c). The effective C^* (Eq. 4) under EQLB conditions compared to CLLPS (EQLB C^*/CLLPS C^*) was a strong function of the compound O : C ratio (Pearson's $r^2 = 0.79$) with higher O : C species having lower EQLB C^* / CLLPS C^* ratios. The mean activity coefficient value was predicted to either stay the same (2-methylglyceric acid) or increase (all other explicit organic species) in EQLB compared to CLLPS. Thus, the driving factor for increased partitioning to the particle phase (indicated by increased F_p and decreased C^*) for species with O : C > 0.6 under EQLB compared to CLLPS was the ability of the increased partitioning medium size to overcome the increased activity coefficients. The increased partitioning medium gained by interacting with the inorganic species and their water lowered the mole fraction of the organic species in the particle, thus leading to lower predicted particle-phase activity and gas-phase concentrations via modified Raoult's law. In some cases, like for 2-methyltetrols, the species exhibited negative deviations from ideality ($\gamma < 1$) in both CLLPS and EQLB, but the activity coefficient still increased from CLLPS to EQLB (Table S9). For pinic and pinonic acid, the deviation ($\gamma > 1$) was positive in CLLPS and its activity coefficient was even larger in magnitude in EQLB such that the larger partitioning medium did not overcome the deviation in ideality, resulting in the species being more abundant in the gas phase in EQLB compared to CLLPS. Interestingly, levoglucosan was the only species predicted to have an activity coefficient near 1 for the organic-rich (β) phase in EQLB calculations (Table S9). Due to the effect on the size of the partitioning medium resulting from additional species (specifically water and inorganic salts) in the β phase during EQLB, the effective C^* for levoglucosan was predicted to be 35% of its pure-species value (1.4 μgm^{-3}, Table S8).

Predicted unfavorable interactions (limited miscibility within both the organic-rich and inorganic-rich liquid phases) resulted in pinonic acid (Fig. 6f) being partitioned to the gas phase to a much greater degree than the measurements indicated. Model performance was consistent with previous work in which multiple measurement techniques showed slightly higher F_p than model predictions (Thompson et al., 2017). Formation of a second organic-rich phase (a third liquid phase) containing lower O : C compounds, which was not allowed in the AIOMFAC calculations, could improve pinonic acid partitioning predictions. The lack of a resolved hydrocarbon-like organic aerosol (HOA) component (Xu et al., 2015a) and representation of its associated functional groups in the model may have also contributed to an unfavorable environment for low O : C compounds.

Overall, the treatment of liquid-phase mixing vs. separation did not improve the mean bias in F_p for the 2-methyltetrol. It also did not significantly change the mean error. The average fraction of 2-methyltetrols in the particles was represented fairly well by assuming half of the measured 2-methyltetrols are actually decomposition products of a fairly nonvolatile (C^* = 10^{-6} µgm^{-3}) dimer compound (dark grey square, Fig. 5a and b). However, this assumption did not perform equally well at all times of day. Figure 6a indicates that the 50% dimer assumption leads to an underestimate in 2-methyltetrol F_p during the day and an overestimate at night. Modeling 2-methyltetrols as entirely monomers with a pure-species C^* of 8 µgm^{-3} at 298.15K (factor of 4.2 reduction in EVAPORATION-predicted vapor pressure) reproduced the daytime 2-methyltetrol partitioning well but overestimated partitioning to the particle at night. Even with the reduced P^{sat} (in the Adj Psat sensitivity), 2-methyletrol monomers remained slightly more volatile than predicted by SIMPOL (C^* = 5 µgm^{-3}) at reference conditions. The average effective 2-methyltetrol C^* (accounting for the effects of temperature and partitioning medium) in the case of CLLPS was 6 µgm^{-3} while in the EQLB calculations it was reduced further to 3.7 µgm^{-3} (Table S8). Thus, 2-methyltetrols behaved like compounds with an effective mean saturation concentration roughly half of the purespecies value due to the influence of temperature and presence of other species in the particle.

4 Conclusions

In this work, conditions over the eastern US were examined with a focus on gas–particle partitioning during the Southern Oxidant and Aerosol Study. Different measurement techniques indicated fairly different ratios of ammonium to $2 \times$ total sulfate, with the AMS instruments having the lowest values, followed by CSN. The MARGA instrument (Allen et al., 2015) and SEARCH network indicated the highest ratios of ammonium to $2 \times$ sulfate of slightly less than 1 (mean of 0.8 to 0.9). The lack of agreement of AMS and CSN data with thermodynamic models, but the agreement between MARGA observations and models, indicates a potential bias in CSN measurements and that AMS data alone may not be suitable for thermodynamic modeling. The diversity in observational data sets can explain why some work has concluded thermodynamic models fail (Silvern et al., 2017) while others indicate models are adequate (Weber et al., 2016). This work finds thermodynamic equilibrium models (both ISORROPIA and AIOMFAC) to be consistent with high ammonium to $2 \times$ sulfate ratios in conjunction with about 70 to 80% of ammonia in the particle. Lower ammonium-to-sulfate ratios imply much higher fractions of total ammonia in the particle as thermodynamic equilibrium assumptions (and models) generally do not allow a large excess of gas-phase ammonia under highly acidic conditions. While consideration of inorganics mixing in liquid phases with organic compounds may increase pH significantly compared to estimates from traditional models like ISORROPIA, that effect is likely not the cause of current inorganic aerosol model evaluation issues.

By performing ISORROPIA and AIOMFAC box modeling, this work demonstrates that our current thermodynamic understanding of ammonium and sulfate aerosol is consistent with (MARGA) observations in the southeastern US atmosphere. Since models like CMAQ use the same thermodynamic basis, specifically ISORROPIA, these results build confidence that regional models can capture the thermodynamics of the ambient atmosphere. However, our

results also demonstrate that for the partitioning of ammonia and ammonium to be correct, errors in emissions of nonvolatile cations, on the order of a factor of 3, must be resolved as well.

AIOMFAC-based predictions of gas–particle partitioning of organic compounds were sensitive to pure-species vapor pressure estimates and predictions generally had a lower mean bias when EVAPORATION-based vapor pressures were adjusted downward by a factor of 4.2 and close to values estimated by SIMPOL for 2-methyltetrols, pinic acid, and hydroxyglutaric acid. The AIOMFAC-based model predicted that organic compounds interact with significant amounts of water and inorganic ions. The 2-methyltetrol predictions had roughly the same error in particle fraction (F_p), assuming 50% of measured particulate 2-methyltetrols were decomposition products or if their vapor pressure was adjusted downward by a factor of 4.2 (to $P^{sat} = 1.4 \times 10^{-4}$ Pa at 298.15 K).

Code and data availability

CMAQ model code is available at https://github.com/USEPA/CMAQ and v5.2-gamma was used in this work. ISORROPIA is available from http://isorropia.eas.gatech.edu/. AIOMFAC can be run online (http://www.aiomfac.caltech.edu/) or via contact with A. Zuend. SOAS data are available at https://esrl.noaa.gov/csd/groups/csd7/measurements/2013senex/. CSN data are available at https://www.epa.gov/outdoor-air-quality-data. Model output associated with the final article will be available from the EPA Environmental Dataset Gateway at https://edg.epa.gov/.

Supplementary Material

Refer to Web version on PubMed Central for supplementary material.

Acknowledgments

References

Allen HM, Draper DC, Ayres BR, Ault A, Bondy A, Takahama S, Modini RL, Baumann K, Edgerton E, Knote C, Laskin A, Wang B, Fry JL. Influence of crustal dust and sea spray supermicron particle concentrations and acidity on inorganic NO3− aerosol during the 2013 Southern Oxidant and Aerosol Study. Atmos Chem Phys. 2015; 15:10669–10685. https://doi.org/10.5194/acp-15-10669-2015.

Appel KW, Pouliot GA, Simon H, Sarwar G, Pye HOT, Napelenok SL, Akhtar F, Roselle SJ. Evaluation of dust and trace metal estimates from the Community Multiscale Air Quality (CMAQ) model version 5.0, Geosci. Model Dev. 2013; 6:883–899. https://doi.org/10.5194/gmd-6-883-2013.

Bahreini R, Ervens B, Middlebrook AM, Warneke C, de Gouw JA, DeCarlo PF, Jimenez JL, Brock CA, Neuman JA, Ryerson TB, Stark H, Atlas E, Brioude J, Fried A, Holloway JS, Peischl J, Richter D, Walega J, Weibring P, Wollny AG, Fehsenfeld FC. Organic aerosol formation in urban and industrial plumes near Houston and Dallas Texas. J Geophys Res. 2009; 114:d00F16. https://doi.org/10.1029/2008JD011493.

Benner CL, Eatough DJ, Eatough NL, Bhardwaja P. Comparison of annular denuder and filter pack collection of $HNO_3(g)$, $HNO_2(g)$, $SO_2(g)$, and particulatephase nitrate, nitrite and sulfate in the south-west desert. Atmos Environ. 1991; 25:1537–1545. https://doi.org/10.1016/0960-1686(91)90013-W.

Bertram AK, Martin ST, Hanna SJ, Smith ML, Bodsworth A, Chen Q, Kuwata M, Liu A, You Y, Zorn SR. Predicting the relative humidities of liquid-liquid phase separation, efflorescence, and deliquescence of mixed particles of ammonium sulfate, organic material, and water using the organic-to-sulfate mass ratio of the particle and the oxygen-tocarbon elemental ratio of the organic component. Atmos Chem Phys. 2011; 11:10995–11006. https://doi.org/10.5194/acp-11-10995-2011.

Budisulistiorini SH, Li X, Bairai ST, Renfro J, Liu Y, Liu YJ, McKinney KA, Martin ST, McNeill VF, Pye HOT, Nenes A, Neff ME, Stone EA, Mueller S, Knote C, Shaw SL, Zhang Z, Gold A, Surratt JD. Examining the effects of anthropogenic emissions on isoprenederived secondary organic aerosol formation during the 2013 Southern Oxidant and Aerosol Study (SOAS) at the Look Rock, Tennessee ground site. Atmos Chem Phys. 2015; 15:8871–8888. https://doi.org/10.5194/acp-15-8871-2015.

Budisulistiorini SH, Nenes A, Carlton AG, Surratt JD, McNeill VF, Pye HOT. Simulating aqueousphase isoprene-epoxydiol (IEPOX) secondary organic aerosol production during the 2013 Southern Oxidant and Aerosol Study (SOAS). Environ Sci Technol. 2017; 51:5026–5034. https://doi.org/10.1021/acs.est.6b05750. [PubMed: 28394569]

Chan MN, Chan AWH, Chhabra PS, Surratt JD, Seinfeld JH. Modeling of secondary organic aerosol yields from laboratory chamber data. Atmos Chem Phys. 2009; 9:5669–5680. https://doi.org/10.5194/acp-9-5669-2009.

Compernolle S, Ceulemans K, Müller JF. EVAPORATION: a new vapour pressure estimation methodfor organic molecules including non-additivity and intramolecular interactions. Atmos Chem Phys. 2011; 11:9431–9450. https://doi.org/10.5194/acp-11-9431-2011.

Eddingsaas NC, VanderVelde DG, Wennberg PO. Kinetics and products of the acid-catalyzed ring-opening of atmospherically relevant butyl epoxy alcohols. J Phys Chem A. 2010; 114:8106–8113. https://doi.org/10.1021/jp103907c. [PubMed: 20684583]

Edgerton ES, Hartsell BE, Saylor RD, Jansen JJ, Hansen DA, Hidy GM. The southeastern aerosol research and characterization study: Part II. Filter-based measurements of fine and coarse particulate matter mass and composition. J Air Waste Manage Assoc. 2005; 55:1527–1542.

Edgerton ES, Hartsell BE, Saylor RD, Jansen JJ, Hansen DA, Hidy GM. The Southeastern Aerosol Research and Characterization Study, Part 3: Continuous measurements of fine particulate matter mass and composition. J Air Waste Manage. 2006; 56:1325–1341.

Fang T, Guo H, Zeng L, Verma V, Nenes A, Weber RJ. Highly acidic ambient particles, soluble metals, and oxidative potential: a link between sulfate and aerosol toxicity. Environ Sci Technol. 2017; 51:2611–2620. https://doi.org/10.1021/acs.est.6b06151. [PubMed: 28141928]

Foroutan H, Young J, Napelenok S, Ran L, Appel KW, Gilliam RC, Pleim JE. Development and evaluation of a physics-based windblown dust emission scheme implemented in the CMAQ modeling system. J Adv Model Earth Syst. 2017; 9:585–608. https://doi.org/10.1002/2016MS000823.

Fountoukis C, Nenes A. ISORROPIA II: a computationally efficient thermodynamic equilibrium model for K+−Ca2+−Mg2+−NH4+−Na+−SO42−−NO3−−Cl−−H2O aerosols. Atmos Chem Phys. 2007; 7:4639–4659. https://doi.org/10.5194/acp-7-4639-2007.

Goldstein AH, Galbally IE. Known and unexplored organic constituents in the Earth's atmosphere. Environ Sci Technol. 2007; 41:1514–1521. https://doi.org/10.1021/es072476p. [PubMed: 17396635]

Guo, H. Hongyu, Guo, et al., editors. Interactive comment on "The underappreciated role of nonvolatile cations on aerosol ammonium-sulfate molar ratios". Atmos Chem Phys Discuss. 2017. https://doi.org/10.5194/acp-2017-737-SC3

Guo H, Xu L, Bougiatioti A, Cerully KM, Capps SL, Hite JR Jr, Carlton AG, Lee S-H, Bergin MH, Ng NL, Nenes A, Weber RJ. Fine-particle water and pH in the southeastern United States. Atmos Chem Phys. 2015; 15:5211–5228. https://doi.org/10.5194/acp-15-5211-2015.

Guo H, Liu J, Froyd KD, Roberts JM, Veres PR, Hayes PL, Jimenez JL, Nenes A, Weber RJ. Fine particle pH and gas–particle phase partitioning of inorganic species in Pasadena, California, during the 2010 CalNex campaign. Atmos Chem Phys. 2017a; 17:5703–5719. https://doi.org/10.5194/acp-17-5703-2017.

Guo, H., Nenes, A., Weber, RJ. The underappreciated role of nonvolatile cations on aerosol ammonium-sulfate molar ratios. Atmos Chem Phys Discuss. 2017b. https://doi.org/10.5194/acp-2017-737, in review

Hansen LD, White VF, Eatough DJ. Determination of gas-phase dimethyl sulfate and monomethyl sulfate. Environ Sci Technol. 1986; 20:872–878. https://doi.org/10.1021/es00151a004. [PubMed: 22263818]

Heath NK, Pleim JE, Gilliam RC, Kang D. A simple lightning assimilation technique for improving retrospective WRF simulations. J Adv Model Earth Sy. 2016; 8:1806–1824. https://doi.org/10.1002/2016MS000735.

Hennigan CJ, Izumi J, Sullivan AP, Weber RJ, Nenes A. A critical evaluation of proxy methods used to estimate the acidity of atmospheric particles. Atmos Chem Phys. 2015; 15:2775–2790. https://doi.org/10.5194/acp-15-2775-2015.

Hettiyadura APS, Jayarathne T, Baumann K, Goldstein AH, de Gouw JA, Koss A, Keutsch FN, Skog K, Stone EA. Qualitative and quantitative analysis of atmospheric organosulfates in Centreville, Alabama. Atmos Chem Phys. 2017; 17:1343–1359. https://doi.org/10.5194/acp-17-1343-2017.

Hu W, Palm BB, Day DA, Campuzano-Jost P, Krechmer JE, Peng Z, de Sá SS, Martin ST, Alexander ML, Baumann K, Hacker L, Kiendler-Scharr A, Koss AR, de Gouw JA, Goldstein AH, Seco R, Sjostedt SJ, Park J-H, Guenther AB, Kim S, Canonaco F, Prévôt ASH, Brune WH, Jimenez JL. Volatility and lifetime against OH heterogeneous reaction of ambient isoprene-epoxydiolsderived secondary organic aerosol (IEPOX-SOA). Atmos Chem Phys. 2016; 16:11563–11580. https://doi.org/10.5194/acp-16-11563-2016.

Hu W, Campuzano-Jost P, Day DA, Croteau P, Canagaratna MR, Jayne JT, Worsnop DR, Jimenez JL. Evaluation of the new capture vaporizer for aerosol mass spectrometers (AMS) through field studies of inorganic species. Aerosol Sci Tech. 2017; 51:735–754. https://doi.org/10.1080/02786826.2017.1296104.

Isaacman G, Kreisberg NM, Yee LD, Worton DR, Chan AWH, Moss JA, Hering SV, Goldstein AH. Online derivatization for hourly measurements of gas- and particlephase semi-volatile oxygenated organic compounds by thermal desorption aerosol gas chromatography (SV-TAG). Atmos Meas Tech. 2014; 7:4417–4429. https://doi.org/10.5194/amt-7-4417-2014.

Isaacman-VanWertz G, Yee LD, Kreisberg NM, Wernis R, Moss JA, Hering SV, de Sá SS, Martin ST, Alexander ML, Palm BB, Hu W, Campuzano-Jost P, Day DA, Jimenez JL, Riva M, Surratt JD, Viegas J, Manzi A, Edgerton E, Baumann K, Souza R, Artaxo P, Goldstein AH. Ambient gas-particle partitioning of tracers for biogenic oxidation. Environ Sci Technol. 2016; 50:9952–9962. https://doi.org/10.1021/acs.est.6b01674. [PubMed: 27552285]

Johnson D, Utembe SR, Jenkin ME, Derwent RG, Hayman GD, Alfarra MR, Coe H, McFiggans G. Simulating regional scale secondary organic aerosol formation during the TORCH 2003 campaign in the southern UK. Atmos Chem Phys. 2006; 6:403–418. https://doi.org/10.5194/acp-6-403-2006.

Kwamena NOA, Buajarern J, Reid JP. Equilibrium morphology of mixed organic/inorganic/aqueous aerosol droplets: investigating the effect of relative humidity and surfactants. J Phys Chem A. 2010; 114:5787–5795. https://doi.org/10.1021/jp1003648. [PubMed: 20408598]

Lopez-Hilfiker FD, Mohr C, D'Ambro EL, Lutz A, Riedel TP, Gaston CJ, Iyer S, Zhang Z, Gold A, Surratt JD, Lee BH, Kurten T, Hu WW, Jimenez J, Hallquist M, Thornton JA. Molecular composition and volatility of organic aerosol in the southeastern U. S.: implications for IEPOX derived SOA. Environ Sci Technol. 2016; 50:2200–2209. https://doi.org/10.1021/acs.est.5b04769. [PubMed: 26811969]

Middlebrook AM, Bahreini R, Jimenez JL, Canagaratna MR. Evaluation of composition-dependent collection efficiencies for the Aerodyne Aerosol Mass Spectrometer using field data. Aerosol Sci Tech. 2012; 46:258–271. https://doi.org/10.1080/02786826.2011.620041.

Nenes A, Pandis SN, Pilinis C. ISORROPIA: A new thermodynamic equilibrium model for multiphase multicomponent inorganic aerosols. Aquat Geochem. 1998; 4:123–152. https://doi.org/10.1023/A:1009604003981.

Nolte CG, Appel KW, Kelly JT, Bhave PV, Fahey KM, Collett JL Jr, Zhang L, Young JO. Evaluation of the Community Multiscale Air Quality (CMAQ) model v5.0 against size-resolved measurements of inorganic particle composition across sites in North America. Geosci Model Dev. 2015; 8:2877–2892. https://doi.org/10.5194/gmd-8-2877-2015.

O'Meara S, Booth AM, Barley MH, Topping D, McFiggans G. An assessment of vapour pressure estimation methods. Phys Chem Chem Phys. 2014; 16:19453–19469. https://doi.org/10.1039/C4CP00857J. [PubMed: 25105180]

Otte TL, Pleim JE. The Meteorology-Chemistry Interface Processor (MCIP) for the CMAQ modeling system: updates through MCIPv3.4.1. Geosci Model Dev. 2010; 3:243–256. https://doi.org/10.5194/gmd-3-243-2010.

Pankow JF, Asher WE. SIMPOL.1: a simple group contribution method for predicting vapor pressures and enthalpies of vaporization of multifunctional organic compounds. Atmos Chem Phys. 2008; 8:2773–2796. https://doi.org/10.5194/acp-8-2773-2008.

Pleim JE, Bash JO, Walker JT, Cooter EJ. Development and evaluation of an ammonia bidirectional flux parameterization for air quality models. J Geophys Res. 2013; 118:3794–3806. https://doi.org/10.1002/jgrd.50262.

Pye HOT, Murphy BN, Xu L, Ng NL, Carlton AG, Guo H, Weber R, Vasilakos P, Appel KW, Budisulistiorini SH, Surratt JD, Nenes A, Hu W, Jimenez JL, Isaacman-VanWertz G, Misztal PK, Goldstein AH. On the implications of aerosol liquid water and phase separation for organic aerosol mass. Atmos Chem Phys. 2017; 17:343–369. https://doi.org/10.5194/acp-17-343-2017.

Reff A, Bhave PV, Simon H, Pace TG, Pouliot GA, Mobley JD, Houyoux M. Emissions inventory of PM2.5 trace elements across the United States. Environ Sci Technol. 2009; 43:5790–5796. https://doi.org/10.1021/es802930x. [PubMed: 19731678]

Reid JP, Dennis-Smither BJ, Kwamena NOA, Miles REH, Hanford KL, Homer CJ. The morphology of aerosol particles consisting of hydrophobic and hydrophilic phases: hydrocarbons, alcohols and fatty acids as the hydrophobic component. Phys Chem Chem Phys. 2011; 13:15559–15572. https://doi.org/10.1039/C1CP21510H. [PubMed: 21811727]

Rindelaub JD, Craig RL, Nandy L, Bondy AL, Dutcher CS, Shepson PB, Ault AP. Direct measurement of pH in individual particles via Raman microspectroscopy and variation in acidity with relative humidity. J Phys Chem A. 2016; 120:911–917. https://doi.org/10.1021/acs.jpca.5b12699. [PubMed: 26745214]

Silvern RF, Jacob DJ, Kim PS, Marais EA, Turner JR, Campuzano-Jost P, Jimenez JL. Inconsistency of ammonium–sulfate aerosol ratios with thermodynamic models in the eastern US: a possible role of organic aerosol. Atmos Chem Phys. 2017; 17:5107–5118. https://doi.org/10.5194/acp-17-5107-2017.

Solomon, PA., Mitchell, W., Tolocka, M., Norris, G., Gemmill, D., Wiener, R., Vanderpool, R., Murdoch, R., Natarajan, S., Hardison, E. Report EPA-454/R-01-005. United States Environmental Protection Agency; Research Triangle Park, NC: 2000. Evaluation of PM2.5 chemical speciation samplers for use in the EPA National PM2.5 Chemical Speciation Network.

Solomon PA, Crumpler D, Flanagan JB, Jayanty RKM, Rickman EE, McDade CE. U.S. national PM2.5 Chemical Speciation Monitoring Networks CSN and IMPROVE: description of networks. J Air Waste Manage. 2014; 64:1410–1438. https://doi.org/10.1080/10962247.2014.956904.

Song M, Marcolli C, Krieger UK, Zuend A, Peter T. Liquid-liquid phase separation in aerosol particles: dependence on O: C, organic functionalities, and compositional complexity. Geophys Res Lett. 2012; 39:L19801. https://doi.org/10.1029/2012GL052807.

Song M, Marcolli C, Krieger UK, Lienhard DM, Peter T. Morphologies of mixed organic/inorganic/aqueous aerosol droplets. Faraday Discuss. 2013; 165:289–316. https://doi.org/10.1039/C3FD00049D. [PubMed: 24601008]

Stockdale A, Krom MD, Mortimer RJG, Benning LG, Carslaw KS, Herbert RJ, Shi Z, Myriokefalitakis S, Kanakidou M, Nenes A. Understanding the nature of atmospheric acid processing of mineral dusts in supplying bioavailable phosphorus to the oceans. P Natl Acad Sci USA. 2016; 113:14639–14644. https://doi.org/10.1073/pnas.1608136113.

Thompson SL, Yatavelli RLN, Stark H, Kimmel JR, Krechmer JE, Day DA, Hu W, Isaacman-VanWertz G, Yee L, Goldstein AH, Khan MAH, Holzinger R, Kreisberg N, Lopez-Hilfiker FD, Mohr C, Thornton JA, Jayne JT, Canagaratna M, Worsnop DR, Jimenez JL. Field intercomparison of the gas/particle partitioning of oxygenated organics during the Southern Oxidant and Aerosol Study (SOAS) in 2013. Aerosol Sci Tech. 2017; 51:30–56. https://doi.org/10.1080/02786826.2016.1254719.

Topping D, Barley M, Bane MK, Higham N, Aumont B, Dingle N, McFiggans G. UManSysProp v1.0: an online and open-source facility for molecular property prediction and atmospheric aerosol calculations. Geosci Model Dev. 2016; 9:899–914. https://doi.org/10.5194/gmd-9-899-2016.

Weber RJ, Guo H, Russell AG, Nenes A. High aerosol acidity despite declining atmospheric sulfate concentrations over the past 15 years. Nat Geosci. 2016; 9:282–285. https://doi.org/10.1038/ngeo2665.

Xu L, Guo H, Boyd CM, Klein M, Bougiatioti A, Cerully KM, Hite JR, Isaacman-VanWertz G, Kreisberg NM, Knote C, Olson K, Koss A, Goldstein AH, Hering SV, de Gouw J, Baumann K, Lee S-H, Nenes A, Weber RJ, Ng NL. Effects of anthropogenic emissions on aerosol formation from isoprene and monoterpenes in the southeastern United States. P Natl Acad Sci USA. 2015a; 112:37–42. https://doi.org/10.1073/pnas.1417609112.

Xu L, Suresh S, Guo H, Weber RJ, Ng NL. Aerosol characterization over the southeastern United States using high-resolution aerosol mass spectrometry: spatial and seasonal variation of aerosol composition and sources with a focus on organic nitrates. Atmos Chem Phys. 2015b; 15:7307–7336. https://doi.org/10.5194/acp-15-7307-2015.

Xu L, Guo H, Weber RJ, Ng NL. Chemical characterization of water-soluble organic aerosol in contrasting rural and urban environments in the southeastern United States. Environ Sci Technol. 2017; 51:78–88. https://doi.org/10.1021/acs.est.6b05002. [PubMed: 27997132]

You Y, Renbaum-Wolff L, Bertram AK. Liquid–liquid phase separation in particles containing organics mixed with ammonium sulfate, ammonium bisulfate, ammonium nitrate or sodium chloride. Atmos Chem Phys. 2013; 13:11723–11734. https://doi.org/10.5194/acp-13-11723-2013.

Yu X-Y, Lee T, Ayres B, Kreidenweis SM, Malm W, Collett JL Jr. Loss of fine particle ammonium from denuded nylon filters. Atmos Environ. 2006; 40:4797–4807. https://doi.org/10.1016/j.atmosenv.2006.03.061.

Zuend A, Seinfeld JH. Modeling the gas-particle partitioning of secondary organic aerosol: the importance of liquidliquid phase separation. Atmos Chem Phys. 2012; 12:3857–3882. https://doi.org/10.5194/acp-12-3857-2012.

Zuend A, Seinfeld JH. A practical method for the calculation of liquid-liquid equilibria in multicomponent organic-water-electrolyte systems using physicochemical constraints. Fluid Phase Equilibr. 2013; 337:201–213. https://doi.org/10.1016/j.fluid.2012.09.034.

Zuend A, Marcolli C, Luo BP, Peter T. A thermodynamic model of mixed organic-inorganic aerosols to predict activity coefficients. Atmos Chem Phys. 2008; 8:4559–4593. https://doi.org/10.5194/acp-8-4559-2008.

Zuend A, Marcolli C, Peter T, Seinfeld JH. Computation of liquid–liquid equilibria and phase stabilities: implications for RH-dependent gas/particle partitioning of organic–inorganic aerosols. Atmos Chem Phys. 2010; 10:7795–7820. https://doi.org/10.5194/acp-10-7795-2010.

Zuend A, Marcolli C, Booth AM, Lienhard DM, Soonsin V, Krieger UK, Topping DO, McFiggans G, Peter T, Seinfeld JH. New and extended parameterization of the thermodynamic model AIOMFAC: calculation of activity coefficients for organic–inorganic mixtures containing carboxyl, hydroxyl, carbonyl, ether, ester, alkenyl, alkyl, and aromatic functional groups. Atmos Chem Phys. 2011; 11:9155–9206. https://doi.org/10.5194/acp-11-9155-2011.
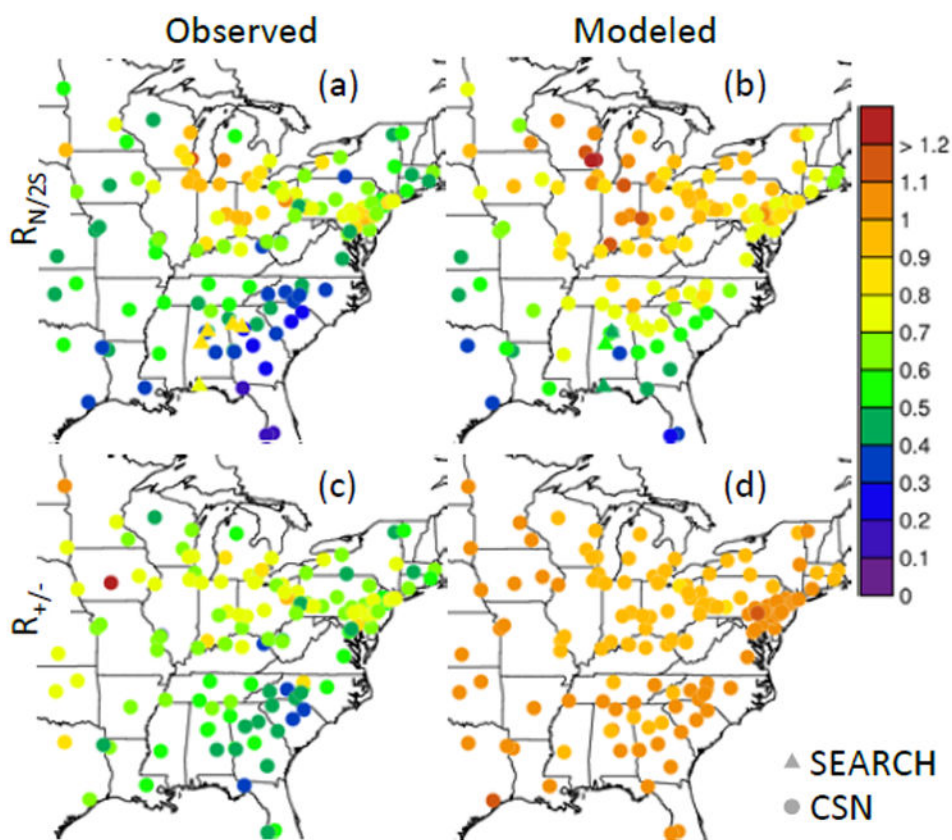
Figure 1.
Molar ratios of aerosol ammonium to 2 × sulfate ($R_{N/2S}$) (**a, b**) and cations to anions ($R_{+/-}$) (**c, d**) over the eastern US for 1 June–15 July 2013 based on observations and predicted by the CMAQ model.
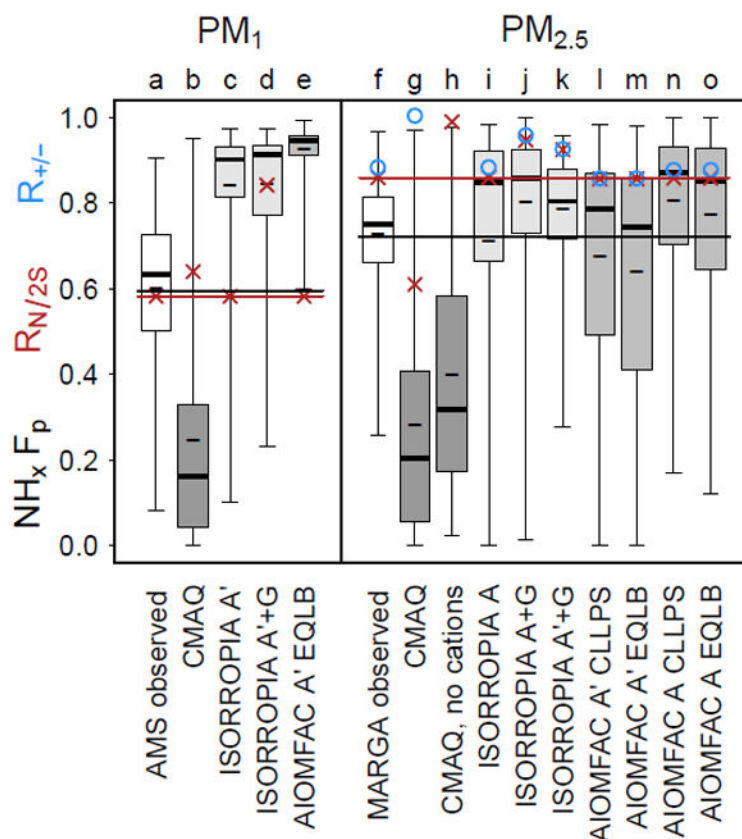
Figure 2.
Gas–particle partitioning of ammonia ($NH_x F_p$ = ammonium/(ammonia + ammonium)),
mean $R_{N/2S}$ (red ×), and mean $R_{+/-}$ (blue ○) for PM_1 measured with the Georgia Tech AMS
(Xu et al., 2015a) and $PM_{2.5}$ measured with a MARGA (Allen et al., 2015) as well as
predicted by a CMAQ regional chemical transport model calculation and box models for
SOAS conditions at CTR. F_p box plots indicate the maximum, 75th percentile, median, 25th
percentile, and minimum. Short dashes within the box plots indicate the mean F_p. Box
model inputs were either the aerosol (A) or aerosol and gas concentrations (A + G). Box
models were run with either the ammonium–sulfate system (A′) or including all cations and
anions (A). AIOMFAC calculations assumed complete liquid–liquid phase separation
between the organic-rich and electrolyte-rich phases (CLLPS) or employed a full
equilibrium calculation with organic compounds in which phase separation was calculated
based on composition (EQLB). Observed gas-phase ammonia concentrations are from the
SEARCH network at CTR. Box plots are labeled by a letter for easier reference in the text.
Shading of the box plot interquartile range distinguishes different models (CMAQ,
ISORROPIA, and AIOMFAC). The horizontal lines correspond to mean observed $NH_x F_p$
(black) and $R_{N/2S}$ (red). A simulation is consistent with observations if it reproduces both
$NH_x F_p$ and $R_{N/2S}$.

Figure 3.
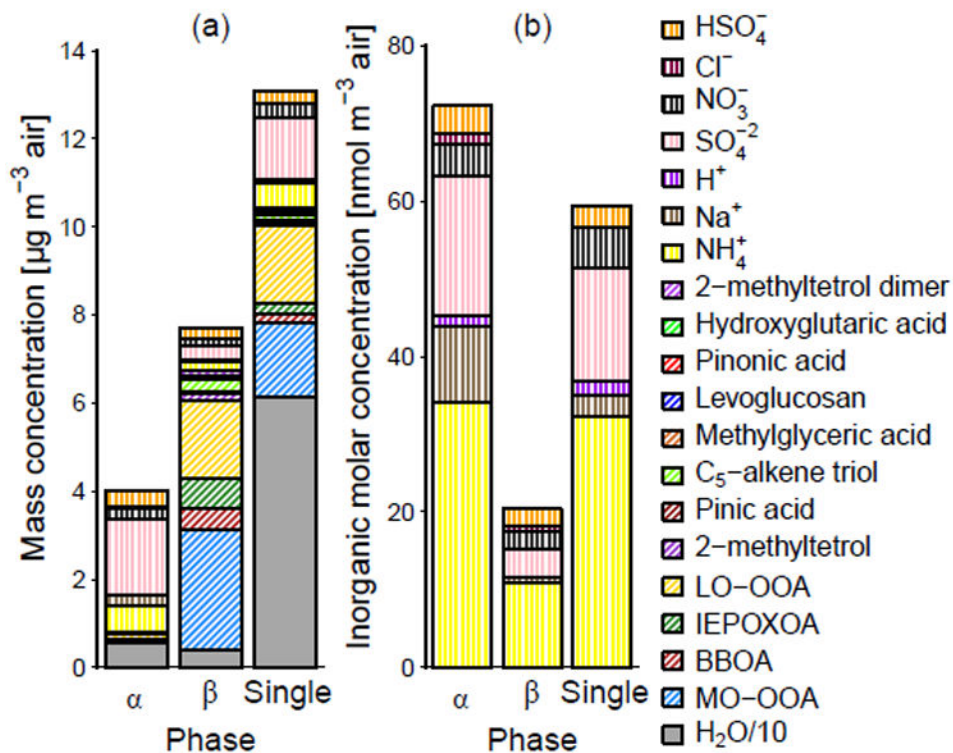Average composition of the α (electrolyte rich), β (organic rich), and single phase in terms of (**a**) mass (organic and inorganic components) and (**b**) moles (ions only) predicted by AIOMFAC using PM$_{2.5}$ aerosol composition observed during SOAS. Species are stacked in the same order as indicated by the legend.

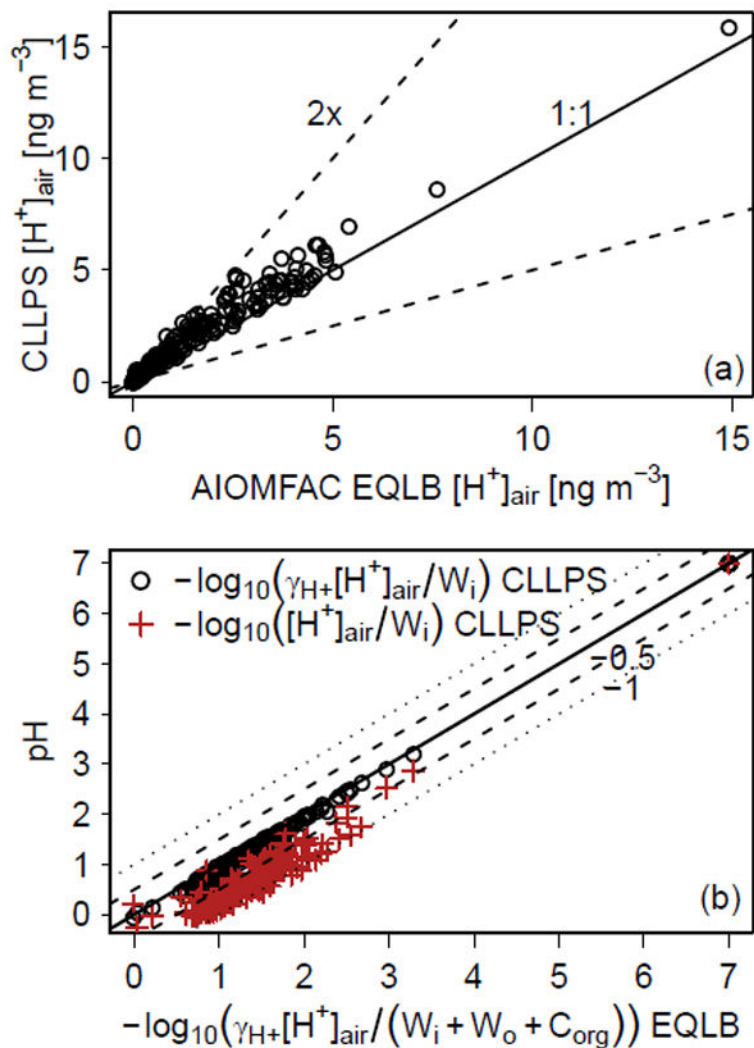**Figure 4.**
(**a**) $[H^+]_{air}$ and (**b**) pH predicted for $PM_{2.5}$ using AIOMFAC. Dashed lines in (**a**) indicate a factor of 2 difference from the 1 : 1 line. Dashed lines in (**b**) represent a ± 0.5 shift in pH while dotted lines represent a ± 1 shift in pH. Series marked in open circles (O) are summarized in Table 1. All calculations used the ammonium–sodium–sulfate–nitrate–chloride and organic compound system.
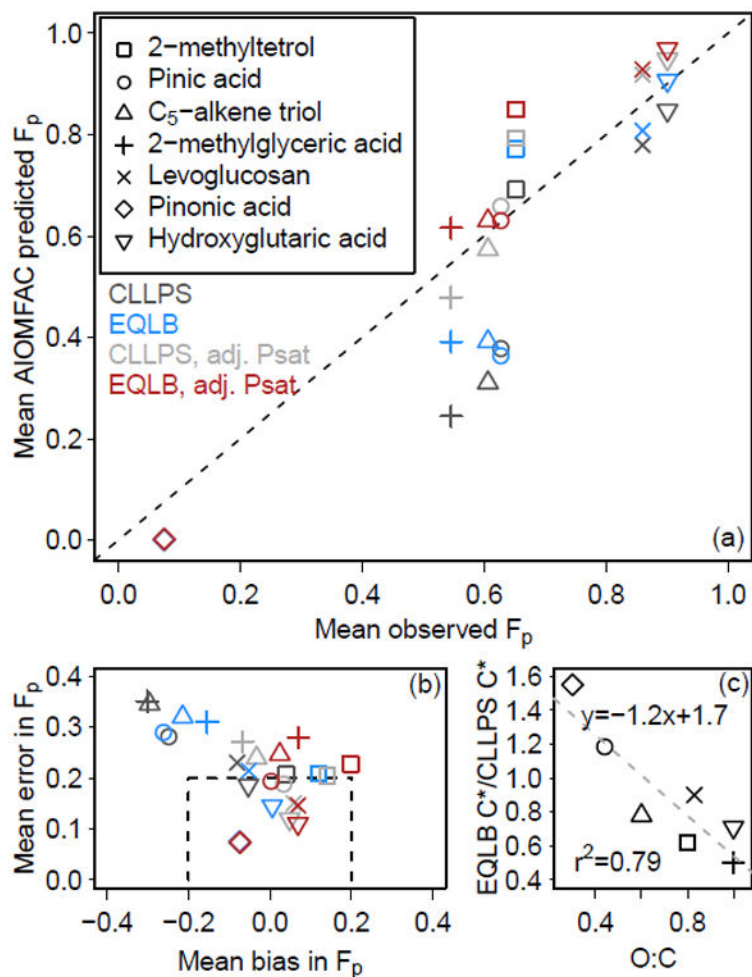
Figure 5.

Observed and predicted equilibrium partitioning of organic compounds in the presence of MARGA-measured $PM_{2.5}$ inorganics, expressed as F_p (**a**). In (**b**),

mean bias $= \frac{1}{n}\sum_{i=1}^{n}(M_i - O_i)$ and mean error $= \frac{1}{n}\sum_{i=1}^{n}|M_i - O_i|$, where M_i is the model prediction and O_i is the observation of F_p. The ratio of mean saturation concentration under EQLB compared to CLLPS conditions (c) uses predictions from the adjusted vapor pressure calculations (Adj Psat). Modeled particulate 2-methyltetrols are 50% dimers except with Adj Psat.
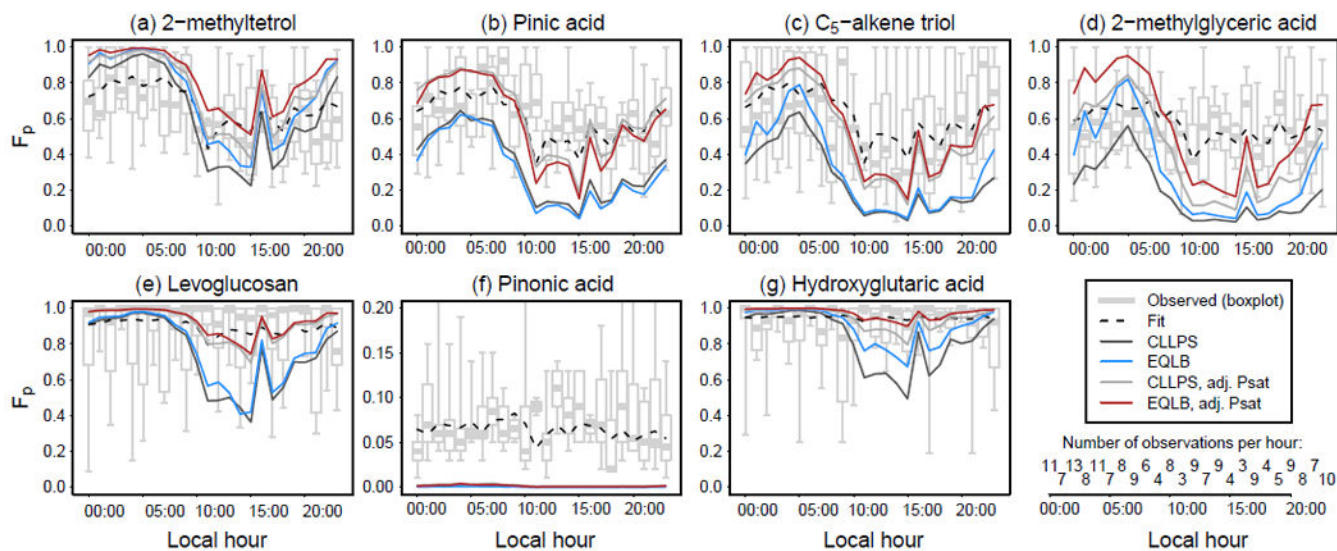
Figure 6.
Fraction of each explicit organic species in the particle as a function of hour of day between 1 June and 15 July 2013 at CTR. The 2-methyltetrols were modeled as 50% dimers in the particle for CLLPS and EQLB. When the pure-species vapor pressure was adjusted, 2-methyltetrols were assumed to be entirely monomers. Fit is based on traditional absorptive partitioning to an organic-compounds-only phase (Eq. S1).

Table 1

$[H^+]_{air}$ and pH predicted for $PM_{2.5}$ at SOAS CTR (median $\pm$ 1 standard deviation) under conditions of complete liquid–liquid phase separation between the organic-rich and electrolyterich phases (CLLPS) or in a full equilibrium calculation in which phase separation was calculated based on composition (EQLB).

Model	CLLPS	EQLB
$[H^+]_{air}$ in nmolm^{-3} air		
AIOMFAC (A$'$)	1.9±1.9	1.3±1.6
AIOMFAC (A)	1.8±2.1	1.1±1.8
ISORROPIA (A)	2.0±2.8	n/a
ISORROPIA (A + G)	0.5±1.5	n/a
pH $= -\log_{10}(\gamma_{H+} [H^+]_{air}/[S])$		
AIOMFAC (A$'$)	1.3±1.2	1.4±1.2
AIOMFAC (A)	1.3±2.1	1.5±2.0
ISORROPIA (A)	0.7±2.5	n/a
ISORROPIA (A + G)	1.1±0.7	n/a

"n/a" means not applicable.